Journal of Molecular Structure 1219 (2020) 128607

Contents lists available at ScienceDirect

Journal of Molecular Structure

journal homepage: http://www.elsevier.com/locate/molstruc

Synthesis, spectroscopic, X-ray diffraction, antimicrobial and antitumor studies of Ni(II) and Co(II) complexes derived from 4-acetyl-5,6-diphenyl-3(2H)-pyridazinone and ethylenediamine

Omima M.I. Adly*, Magdy Shebl, Ebtesam M. Abdelrhman, B.A. El-Shetary

Department of Chemistry, Faculty of Education, Ain Shams University, Roxy, Cairo, Egypt

ARTICLE INFO

Article history:
Received 4 May 2020
Received in revised form
1 June 2020
Accepted 2 June 2020
Available online 7 June 2020

Keywords:
Pyridazinone
Tetradentate ligand
Mono- and binuclear complexes
Antimicrobial activity
Antitumor activity

ABSTRACT

Reactions of the Schiff base ligand derived from 4-acetyl-5,6-diphenyl-3(2H)-pyridazinone and ethylenediamine with Ni(II) and Co(II) using different metal salts; NO_3^-, AcO^-, ClO_4^- and Cl^- yielded binary metal complexes. Mixed-ligand complexes were synthesized by using extra ligands including 8-hydroxyquinoline or glycine as nitrogen, oxygen-donors; 1,10-phenanthroline or 2-aminopyridine as nitrogen, nitrogen-donors. Elemental and thermal analyses, spectroscopic techniques (IR, electronic and mass), conductivity and magnetic susceptibility measurements were utilized to characterize the structures of the complexes. Electronic spectra and magnetic moment measurements showed that all complexes are octahedral and tetrahedral. In addition, activation energies of thermal degradation were calculated by means of Coats–Redfern equations. The activation energies were also used to evaluate kinetic and thermodynamic parameter of the metal complexes including Ea, ΔH, ΔS and ΔG. The XRD patterns for the ligand and its metal complexes indicate crystalline nature with nano particle sizes. The biological activity of the chelating agent and its metal complexes was conducted towards *S. aureus* and *B. subtilis* as Gram-+ve bacteria, *S. typhimurium* and *E. coli* as Gram–-ve bacteria, *C. albicans* (yeast) and *A. fumigatus* (fungus). The chelating agent and some Ni(II) and Co(II) complexes showed antitumor activity towards HepG2 cell line.

1. Introduction

Schiff bases represent the most important chelating agents (ligands) in coordination chemistry. Schiff bases and their metal complexes revealed diverse medicinal applications such as anticancer [1–3], antitumor [4], anti-inflammatory [5], antioxidant [6,7], antimycobacterial [8], antimicrobial [9,10], antibacterial [11], antifungal activities [12] as well as DNA binding affinity [13]. Pyridazine derivatives as 1,2-diazines are interested heterocycles due to their various biological activity including anticancer [14,15], antiviral [16], anti-HIV [17], antitubercular [18], anti-leishmanial [19], anti-inflammatory [20], anticonvulsant [21], antihypertensive [22] antimicrobial [23], antifungal [24], and analgesic [25] activities.

Mixed-ligand complexes have attracted a considerable interest as a result of their vital function in biological processes. Indded, they serve as appropriate models for valuable information in the clarification of enzymatic processes of biological significance [26,27]. In our previous article [28], a new Schiff base ligand identified as N,N′-*bis*[5,6-diphenyl-3-oxo-2*H*-pyridazin-3-ylethylidene]ethane-1,2-diamine was prepared and its coordinating behavior towards different copper(II) salts was explored. Different modes of bonding were observed in these complexes in addition to their promising biological activities towards selected organisms [28]. Herein, the present work aims to study the chelating behavior of this Schiff base ligand towards a variety of Ni(II) and Co(II) ions. Mono-, binuclear and mixed-ligand complexes have been successfully prepared and characterized by analytical and spectral techniques, molar conductivity and magnetic susceptibility measurements and thermal analysis. The biological activity of the ligand and Ni(II) and Co(II)- complexes was conducted towards different types of bacteria and fungi. The chelating agent [28] and some Ni(II) and Co(II) complexes showed antitumor activity towards HepG2 cell line.

* Corresponding author.
E-mail address: omima_adly@yahoo.com (O.M.I. Adly).

https://doi.org/10.1016/j.molstruc.2020.128607
0022-2860/

2. Experimental

2.1. Measurements

Microanalyses (Carbon, Hydrogen and Nitrogen) were performed using Vario El-Elementar analyzer. Nickel and cobalt content was estimated by EDTA complexometrically after decomposition of the chelates with conc. nitric acid. Melting point of the chelates were measured by a Stuart SMP3 melting point apparatus. Infra-red spectra were recorded using potassium bromide discs on FT-IR Nicolet IS10 spectrometer. Electronic spectra were recorded on a JASCO model V-550 UV/Vis spectrophotometer as Nujol mulls and/or solutions in DMF. Mass spectra were recorded at 70 eV on a Gas chromatographic GCMSqp 1000 ex Shimadzu instrument. The magnetic susceptibility measurements were performed at room temperature using a Johnson Matthey magnetic susceptibility balance (Alfa product). The calculated magnetic moment values were corrected using Pascal's constants [29]. Molar conductivities of complexes solutions were measured by the Corning conductivity meter NY 12631 (model 441). A Shimadzu-50 instrument was used to record TG. The XRD patterns were recorded using PHILIPS diffractometer with CuKα1 radiation ($\lambda = 1.54056$ Å). The accelerating voltage of 40 kV and an emission current of 30 mA were applied.

2.2. Materials

Following literature method [28,30], 4-acetyl-5,6-diphenyl-3(2H)-pyridazinone was synthesized. Metal(II) salts (acetate, nitrate, sulphate, chloride and perchlorate), 8-hydroxyquinoline (8-HQ), 1,10-phenanthroline (Phen), glycine (Gly), 2-aminopyridine (2-Ampy), Na_2EDTA, ammonium hydroxide, metal indicators and nitric acid were either Merck, BDH or Aldrich products. Organic solvents were reagent grade chemicals and were employed without extra purification.

2.3. Synthesis of the Schiff base ligand

The Schiff base ligand was prepared according to our previous work [28].

2.4. Synthesis of the metal complexes

The pyridazinone ligand (in ethanol) was mixed with the nickel(II) or cobalt(II) salts (in ethanol) in the molar ratio 2:1 (M:L) and refluxed for ~6 h. The obtained precipitates were filtered, washed with ethanol then Et_2O and lastly stored in a desiccator over anhydrous $CaCl_2$.

2.4.1. $[Co(L)(OAc)_2].H_2O$ (7)

To ~0.8 g (1.32 mmol) of the Schiff base ligand in ~50 mL ethanol, 0.658 g (2.64 mmol) of cobalt(II) acetate tetrahydrate in ~50 mL ethanol was added with stirring. The mixture was refluxued for ~6 h. A brown precipitate was formed. After cooling, the precipitate was filtered off, washed with ethanol then Et_2O and dried. The yield was 51% and m.p. 210 °C.

2.4.2. $[Co_2(L)(OAc)_2(8\text{-}HQ)_2(H_2O)_2]$ (9)

To ~2 g (3.3 mmol) of the Schiff base ligand in ~100 mL ethanol, ~1.64 g (6.6 mmol) of cobalt(II) acetate tetrahydrate in ~100 mL ethanol was added with stirring. The mixture was refluxed for ~1 h. then (6.6 mmol) of 8-hydroxyquinoline was added to the exceeding mixture. The resulting mixture was refluxed for ~6 h. A dark green precipitate was formed. After cooling, the precipitate was filtered off, washed with ethanol then Et_2O and dried. The yield was 44% and m.p. <300 °C.

2.4.3. Failed experiments

All experiments to synthesize the binary Ni(II) and Co(II) Schiff base complexes by using Ni(II) and Co(II) sulphates were failed.

2.5. Biological activity

2.5.1. Antimicrobial activity

By using the standardized disc-agar diffusion technique [31], the antimicrobial activity of the pyridazinone ligand and its Ni(II) and Co(II) complexes was explored towards Gram -ve bacteria *(S. typhimurium* and *E. coli)*, Gram +ve bacteria (*S. aureus* and *B. subtilis)* and *C. albicans* and *A. fumigatus* (fungus). Cephalothin was utilized as a control for Gram -ve bacteria, chloramphenicol for Gram +ve bacteria and cycloheximide for fungi.

2.5.2. Antitumor activity

On the basis of the literature method [32], the antitumor activity of the synthesized chelates was checked on Hep G2 cells by determining the effect of the test samples on cell morphology and cell viability.

3. Results and discussion

3.1. General

The pyridazinone ligand reacted with different Ni(II) and Co(II) salts; acetate, chloride, nitrate and perchlorate to examine the effect of the anion on the complexation process. Furthermore, the pyridazinone ligand reacted with metal acetate in the presence of auxiliary ligands; 8-hydroxyquinoline, glycine as nitrogen, oxygen-donors and 1,10-phenanthroline and 2-aminopyridine as nitrogen, nitrogen-donors. The prepared complexes are sparingly soluble in H_2O and familiar organic solvents. Characterization of the prepared complexes was achieved by analytical and spectral techniques. Table 1 lists the results of elemental analyses and physical properties of the complexes.

3.1.1. IR spectra

Table 2 summarizes the main infra-red spectroscopic data of the complexes. A strong broad band in the range 3381–3446 cm^{-1} was observed in the IR spectra of the metal complexes, which may be ascribed to ν(OH) of the coordinated or non-coordinated water and ethanol molecules linked to complexes. The strong bands attributed to ν(C=O) and ν(C=N), in the free Schiff base, were shifted to lower wave number in the complexes, signifying the contribution of these groups in complexation [33]. The band assigned to ν(NH) was observed in the range 3128–3346 cm^{-1}. The two bands attributed to ν(NH) and ν(C=O) appeared in the infra-red spectra of the complexes, pointing to the existence of the Schiff base in the pyridazinone form in the complexes [28]. The mode of bonding of the anions present in the complexes was explained by the IR spectral data and confirmed by molar conductivity measurerments. In complexes **1**, **4**–**7**, **9** and **12** (acetato complexes), the new bands appeared in the ranges 1424-1489 and 1212-1239 cm^{-1} may be related to $\nu_{asymmetric}$ (COO^-) and $\nu_{symmetric}$ (COO^-), respectively, of the acetate ligand [34]. The calculated band difference ($\Delta\nu = (\nu_{asymmetric} - \nu_{symmetric}) = 212\text{-}250$ cm^{-1}) points to a monodentate behavior of the acetate anion [34,35], while complexes **10** and **11** showed new bands observed at (1575, 1439 and 833) cm^{-1} for complex **10** and (1577, 1433 and 853) cm^{-1} for complex **11**, indicating the ionic character of the acetate group [34]. The new bands observed at 1378 and 830 cm^{-1} in complex **2** may be due to the ionic nitrate group [36,37] while those observed at 1091 and

Table 1
Analytical and physical data of the Schiff base and its complexes.

No.	Complex	M. F. [F. Wt]	Color	Yield (%)	M.P. °C	Elemental analysis, % Found/(Calc.)				
						C	H	N	Cl/Br	M
1	$[Ni_2(L)(OAc)_4(H_2O)_2(EtOH)_2].1.5H_2O$	$C_{50}H_{63}N_6O_{15..5}Ni_2$ [1115.46]	Pale green	61.60	>300	53.30 (53.84)	5.30 (5.69)	7.27 (7.53)		10.72 (10.70)
2	$[Ni(L)](NO_3)_2$	$C_{38}H_{32}N_8O_8Ni$ [787.62]	Green	67.42	230	57.20 (57.90)	4.15 (4.09)	14.52 (14.23)		7.59 (7.47)
3	$[Ni(L)(H_2O)_2](ClO_4)_2$	$C_{38}H_{36}N_6O_{12}Cl_2Ni$ [898.43]	Green	50.00	[a]	50.32 (50.80)	4.40 (4.00)	8.60 (9.35)	(7.59)	[a] (6.53)
4	$[Ni_2(L)(OAc)_2(8\text{-}HQ)_2(H_2O)_2].0.5EtOH$	$C_{61}H_{57}N_8O_{10.5}Ni_2$ [1187.56]	Green	35.00	>300	61.50 (61.69)	4.72 (4.83)	9.22 (9.43)		9.90 (9.88)
5	$[Ni_2(L)(OAc)_4(Phen)_2]$	$C_{70}H_{60}N_{10}O_{10}Ni_2$ [1318.69]	Pale green	56.04	285	63.36 (63.80)	5.13 (4.58)	10.35 (10.62)		8.39 (8.90)
6	$[Ni_2(L)(OAc)_4(2\text{-}Ampy)_2(H_2O)_2].2.5H_2O$	$C_{56}H_{65}N_{10}O_{14.5}Ni_2$ [1227.59]	Green	64.63	>300	54.64 (54.79)	5.66 (5.33)	11.87 (11.41)		9.83 (9.56)
7	$[Co(L)(OAc)_2].H_2O$	$C_{42}H_{40}N_6O_7Co$ [799.68]	Brown	51.00	280	62.95 (63.08)	5.44 (5.04)	9.72 (10.21)		7.90 (7.36)
8	$[Co(L)Cl_2]$	$C_{38}H_{32}N_6O_2\ Cl_2Co$ [734.61]	Green	61.74	245	62.27 (62.13)	4.67 (4.39)	10.92 (11.44)	(9.66)	8..97 (8.02)
9	$[Co_2(L)(OAc)_2(8\text{-}HQ)_2(H_2O)_2]$	$C_{60}H_{54}N_8O_{10}Co_2$ [1164.93]	Reddish brown	43.60	>300	61.96 (61.86)	4.68 (4.67)	9.06 (9.61)		10.00 (10.11)
10	$[Co(L)(Gly)](OAc).2H_2O$	$C_{43}H_{45}N_7O_8Co$ [846.53]	Reddish brown	52.85	231	61.31 (61.01)	4.95 (5.35)	10.73 (11.58)		6.94 (6.93)
11	$[Co(L)(Phen)](OAc)_2$	$C_{54}H_{46}N_8O_6Co$ [961.89]	Orange	68.86	284	67.46 (67.42)	4.93 (4.81)	11.21 (11.64)		6.71 (6.12)
12	$[Co_2(L)(OAc)_4(2\text{-}Ampy)_2(H_2O)_2].2H_2O$	$C_{56}H_{64}N_{10}O_{14}Co_2$[1218.98]	Brown	59.84	263	55.41 (55.17)	4.84 (5.29)	11.22 (11.49)		9.19 (9.66)

[a] not determined.

Table 2
Characteristic IR spectral data of the Schiff base and its complexes.

IR Spectra $(cm)^{-1}$									
No.	Complex	ν(OH)	ν(NH)	ν(C═O)	ν(C═N)	ν(C═C)	ν(M-O)	ν(M-N)	Other bands
	L	–	3289	1665	1572	1537	–	–	
1	$[Ni_2(L)(OAc)_4(H_2O)_2(EtOH)_2].1.5\text{-}H_2O$	3443	3128	1643	1567	1507	522	439	1489$\nu_{as}(COO^-)$, 1212$\nu_s(COO^-)$; (mondentate OAc^-)
2	$[Ni(L)](NO_3)_2$	–	3165	1642	1510	1510	526	477	1378, 830; $\nu(NO_3^-)$ (ionic)
3	$[Ni(L)(H_2O)_2](ClO_4)_2$	3424	3316	1635	1521	1521	521	429	1091, 622; $\nu(ClO_4^-)$ (ionic)
4	$[Ni_2(L)(OAc)_2(8\text{-}HQ)_2(H_2O)_2].0.5EtOH$	3381	3195	1641	1501	1499	608	434	1465$\nu_{as}(COO^-)$, 1239$\nu_s(COO^-)$; (mondentate OAc^-), 1499; ν(C═N) 8-HQ
5	$[Ni_2(L)(OAc)_4(Phen)_2]$	–	3217	1641	1563	–	521	489	1424$\nu_{as}(COO^-)$, 1218$\nu_s(COO^-)$; (mondentate OAc^-) 1510; ν(C═N) Phen
6	$[Ni_2(L)(OAc)_4(2\text{-}Ampy)_2(H_2O)_2].2.5H_2O$	3420	3227	1644	1560	1496	522	431	1424$\nu_{as}(COO^-)$, 1216$\nu_s(COO^-)$; (mondentate OAc^-), 925; ν(2-Ampy)
7	$[Co(L)(OAc)_2].H_2O$	3424	3242	1646	1560	1491	515	473	1454$\nu_{as}(COO^-)$, 1218$\nu_s(COO^-)$; (mondentate OAc^-)
8	$[Co(L)Cl_2]$	–	3260	1635	1521	1521	510	423	
9	$[Co_2(L)(OAc)_2(8\text{-}HQ)_2(H_2O)_2]$	3425	3304	1641	1543	1495	543	434	1462$\nu_{as}(COO^-)$, 1217$\nu_s(COO^-)$; (mondentate OAc^-); 1496ν(C═N) 8-HQ
10	$[Co(L)(Gly)](OAc).2H_2O$	3446	3303	1640	1540	1490	515	419	1575, 1439, 833; (ionic OAc^-) 1374; νs(COO^-) Gly
11	$[Co(L)(Phen)](OAc)_2$	–	3277	1640	1520	1522	533	433	1577, 1433, 853; (ionic OAc^-), 1520; ν(C═N) Phen
12	$[Co_2(L)(OAc)_4(2\text{-}Ampy)_2(H_2O)_2].2H_2O$	3446	3346	1637	1560	1492	515	419	1438$\nu_{as}(COO^-)$, 1214$\nu_s(COO^-)$; (mondentate OAc^-), 919; ν(2-Ampy)

622 cm^{-1} in complex **3** may be attributed to the ionic perchlorate group [38–40]. The new bands observed in the IR spectra of the complexes (**4**, **5**, **9** and **11**) in the range 1496–1520 cm^{-1} may be attributed to ν(C═N) of the secondary ligand, confirming formation of ternary complexes [41,42]. Complex (**10**) exhibited a new band at 1374 cm^{-1}, which may be attributed to $\nu_{symmetric}$ (COO^-) of the glycine moiety [43,44]. Unfortunately, $\nu_{asymmetric}(COO^-)$ of glycine was masked by the high intensity C═C band [43,45]. Complexes (**6**, **12**) exhibited new bands at 925 and 919 cm^{-1}, respectively which may be due to pyridine ring of 2-aminopyridine [46]. Finally, metal-oxygen and metal-nitrogen bands were observed in the ranges 510-608 and 419-489 cm^{-1}, respectively [47].

3.1.2. Conductivity measurements

The molar conductance values of the complexes-listed in Table 3- illustrated the non-electrolytic character of all complexes excluding complexes **2**, **3** and **11** (molar conductance values = 117, 115 and 118 Ω^{-1} cm^2 mol^{-1}, respectively), signifying their 1:2 electrolytic character and complex **10** (molar conductivity value = 73 Ω^{-1} cm^2 mol^{-1}) signifying its 1:1 electrolytic character [48]. These results are consistent with the infrared spectral data (item 3.1.1) that proved the presence of ionic acetate, nitrate and perchlorate groups in the cationic complexes. The partial dissociation in their dimethylformamide solutions [48], may be the reason for the fairly high conductivity values of complexes **5** and **6**.

3.1.3. Magnetic moment measurements and electronic spectra

The room-temperature magnetic moments of the Ni(II) complexes **1**, **5** and **6** (Table 3) are in the range (2.15–2.83) B.M., which lie below the range (2.9–3.3) B.M. of the octahedral Ni(II) complexes [49]. This subnormal magnetic moment values may be due to anti-ferromagnetic interaction [50]. Conversely, complexes **3** and **4** have magnetic moment values 3.38 and 3.34 B.M., respectively which are slightly higher than the range (2.9–3.3) B.M. of the octahedral Ni(II) complexes, indicating spin-orbit coupling. The magnetic moment value of complex **2** is 2.78 B.M., which is below the range (3.2–4.1 B.M) of the tetrahedral Ni(II) complexes, indicating anti-ferromagnetic interaction [49].

The electronic spectrum of Ni(II) complex **5** exhibited two bands at 525 and 750 nm, which may be related to $^3A_{2g}(F) \rightarrow {}^3T_{1g}(P)$ and $^3A_{2g}(F) \rightarrow {}^3T_{1g}(F)$ transitions, respectively in an octahedral geometry [52], while in complexes **1, 3, 4** and **6** one band was observed in the range (597-750) nm, which may be assigned to $^3A_{2g}(F) \rightarrow {}^3T_{1g}(F)$ transition [49]. However, complex **2** exhibited an absorption

Table 3
Electronic spectra, magnetic moments and molar conductivity data of the Schiff base and its complexes.

No.	Complex	Electronic spectral bands[a] (nm) λ_{max}[a] (nm)/[ε_{max} L cm^{-1} mol^{-1}]	$\mu_{eff.}$[d] B.M.	$\mu_{compl.}$[e] B.M.	Conductance[a] (Ω^{-1} cm^2 mol^{-1})
	L	271 [1.04], 328 [0.32]	–		–
1	$[Ni_2(L)(OAc)_4(H_2O)_2(EtOH)_2].1.5H_2O$	(642)[b]	2.33	3.29	7.67
2	$[Ni(L)](NO_3)_2$	(567)[b] (608)[c]	2.78	–	117.00
3	$[Ni(L)(H_2O)_2](ClO_4)_2$	(640)[b] (629)[c]	3.38	–	115.00
4	$[Ni_2(L)(OAc)_2(8\text{-}HQ)_2(H_2O)_2].0.5EtOH$	(612)[b] (604)[c]	3.34	5.05	4.66
5	$[Ni_2(L)(OAc)_4(Phen)_2]$	(525,750)[c]	2.15	3.05	22.08
6	$[Ni_2(L)(OAc)_4(2\text{-}Ampy)_2(H_2O)_2].2.5H_2O$	(599)[b] (597)[c]	2.83	3.99	17.34
7	$[Co(L)(OAc)_2].H_2O$	(565)[b] (408, 591)[c]	3.00	–	6.31
8	$[Co(L)Cl_2]$	(408, 634)[b] (414, 605, 666)[c]	4.31	–	6.81
9	$[Co_2(L)(OAc)_2(8\text{-}HQ)_2(H_2O)_2]$	(435, 558)[c]	5.2	7.38	4.69
10	[Co(L)(Gly)](OAc).2H$_2$O	(410, 537)[b]	3.00	–	73.00
11	$[Co(L)(Phen)](OAc)_2$	(525)[b]	4.70	–	118.00
12	$[Co_2(L)(OAc)_4(2\text{-}Ampy)_2\ (H_2O)_2].2H_2O$	(425, 561)[b] (434, 554)[c]	4.26	6.02	10.01

[a] Solutions in DMF (10^{-3} M); Values of ε_{max} are in square brackets and multiplied by 10^{-4}.
[b] Nujol mull.
[c] Concentrated solutions.
[d] $\mu_{eff.}$ is the magnetic moment of one cationic species in the complex.
[e] $\mu_{compl.}$ is the total magnetic moments of all cations in the complex.

band at 608 nm, which may be assigned to $^3T_{1g}(F) \rightarrow {}^3T_{1g}(P)$ transition, which could occur in a tetrahedral d^8 arrangement [50,53]. Thus, in the light of magnetic moments and electronic spectral data, Ni(II) complexes have octahedral and tetrahedral geometries with their characteristic features.

The effective magnetic moment of the Co(II) complexes **9** and **11** are 5.2 and 4.7 B.M., respectively, indicating octahedral Co(II) complexes [54]. Complexes **7**, **8**, **10** and **12** have subnormal magnetic moment values which lie in the range (3–4.31) B.M., which may be due to anti-ferromagnetic interaction [55].

The electronic spectra of the Co(II) complexes (**7, 9–12)** exhibited one band in the range (525-605) nm, which may be assigned to $^4T_{1g}(F) \rightarrow {}^4T_{1g}(P)$ transition in octahedral geometry [56]. In case of complex **8**, two bands were observed, the former band may be due to $^4T_{1g}(F) \rightarrow {}^4A_{2g}(F)$ transition, which was observed at 666 nm. The second band may be due to $^4T_{1g}(F) \rightarrow {}^4T_{1g}(P)$ transition, which was observed at 605 nm, indicating octahedral geometry. In most complexes another band was observed in the range (408-435) nm, which may be due to charge transfer.

3.1.4. Thermal analysis

Usually, TGA is used to inspect the character of H_2O or solvent molecules–associated with the complexes-to be either in the internal or external coordination sphere of the metal ion [57]. In the current study, complexes **1**, **4, 6, 7, 9** and 12 were taken as ambassador examples (Table 4).

The thermogram of complex **1**, $[Ni_2(L)(OAc)_4(H_2O)_2(EtOH)_2].1.5H_2O$ (Fig. 1) displayed three steps of degradation within 57–506 °C range. The first one (57–147 °C) corresponds to elimination of one and half non-coordinated H_2O molecule (weight loss; Calc./Found%; 2.29/2.42%). The second step (147–320 °C) is related to elimination of two coordinated C_2H_6OH molecules and two coordinated H_2O molecules (weight loss; Calc./Found%; 11.45/12.15%). The third step (320–506 °C) corresponds to the elimination of four AcOH molecules and $C_6H_{10}N_6$ molecule (weight loss; Calc./Found%; 38.48/38.27%). The thermogram of complex **4**, $[Ni_2(L)(OAc)_2(8\text{-}HQ)_2(H_2O)_2].0.5EtOH$ (Fig. 2), displayed three steps of degradation within 47–324 °C range. The first (47–80 °C) is related to the elimination of half non-coordinated C_2H_5OH molecule (weight loss; Calc./Found%; 1.95/1.60%). The second step (80–196 °C) corresponds to the loss of one AcOH molecule and two coordinated H_2O molecules (weight loss; Calc./Found%; 8.18/7.80%). The third step (196–324 °C) corresponds to the elimination of one AcOH molecule (weight loss; Calc./Found%; 5.11/6.21%). The thermogram of complex **7**, $[Co(L)(OAc)_2].H_2O$, displayed two steps of degradation within 49–298 °C range. The first one (49–149 °C) corresponds to the elimination of one non-coordinated H_2O molecule (weight loss; Calc./Found%; 2.25/2.82%). The second one (149–298 °C) is related to the elimination of one AcOH molecule and C_2H_6 molecule (weight loss; Calc./Found%; 13.25/11.88%). The thermogram of complex (**12**), $[Co_2(L)(OAc)_4(2\text{-}Ampy)_2(H_2O)_2].2H_2O$ (Fig. 3), displayed two steps of degradation within 44–296 °C range. The first one (44–132 °C) is related to the removal of two non-coordinated H_2O molecules (weight loss; Calc./Found%; 3.22/3.65%). The second step (132–296 °C) corresponds to the loss of four AcOH molecules and two coordinated H_2O molecules (weight loss; Calc./Found%; 24.66/23.48%).

The Coats–Redfern method [58] was used to find out the influence of the nature of the metal on the thermal behavior of the complexes and the activation parameters of the different decomposition stages. The kinetic parameters are summarized in Table 5. As expected, Ea, ΔH, ΔG values are positive, whereas ΔS are negative, which indicating non–spontanous process of the thermal decomposition of the complexes.

The activation energy E_a values of the metal complexes show that the thermal stability of second step of decomposition of all complexes are smaller than the first stage. This shows that the rate of decomposition for this stage is greater than the first stage [59]. In addition, the positive values of ΔH* means that the decomposition processes are endothermic.

The negative values of ΔS* of thermal decomposition of the complexes is more ordered than the reactants and/or the reactions are slow [60]. The positive ΔG values suggested that non–spontaneous processes. the obtained energy values of the thermal decomposition pattern of the complexes revealed that these materials have ahigh thermal stability this is due to the covalent character of their bonds [61].

Table 4
Thermal analysis data of some metal complexes.

Complex	DTG peak (°C)	Temperature range (°C)	% Wt. loss Found/ (Calc.)	Lost fragment (No. of molecules)
$[Ni_2(L)(OAc)_4(H_2O)_2(EtOH)_2].1.5H_2O$ **(1)**	95	57–147	2.42 (2.29)	
	251	147–320	12.15 (11.45)	-
	448	320–506	38.27 (38.48)	One and half lattice water
				-
				two coordinated ethanol molecules + two coordinated water molecules
				-
				Four CH_3COOH molecules + $C_6H_{10}N_6$ molecule
$[Ni_2(L)(OAc)_2(8\text{-}HQ)_2(H_2O)_2].0.5EtOH$	70	47–80	1.60 (1.95)	
(4)	162	80–196	7.80 (8.18)	-
	245	196–324	6.21 (5.11)	Half lattice ethanol molecule
				-
				Two coordinated water molecules + one CH_3COOH molecule
				-
				One CH_3COOH molecule
$[Ni_2(L)(OAc)_4(2\text{-}Ampy)_2(H_2O)_2].2.5H_2O$	100	45–139	3.65 (3.66)	- Two and half lattice water molecules
(6)	216	139–310	22.00 (21.7)	- Two coordinated water molecules + four CH_3COOH molecules
$[Co(L)(OAc)_2].H_2O$ **(7)**	94	49–149	2.82 (2.25)	- One lattice water molecule
	223	149–298	11.88 (13.25)	- One CH_3COOHmolecule + C_2H_6 molecule
$[Co_2(L)(OAc)_2(8\text{-}HQ)_2(H_2O)_2]$ **(9)**	258	154–339	3.09 (2.43)	- One coordinated water molecule
	436	339–480	10.30 (9.88)	- One coordinated water molecule + one CH_3COOH molecule
$[Co_2(L)(OAc)_4(2\text{-}Ampy)_2(H_2O)_2].2H_2O$	90	44–132	3.65 (3.22)	- Two lattice water molecules
(12)	207	132–296	23.48 (24.66)	- Two coordinated water molecules + four CH_3COOH molecules

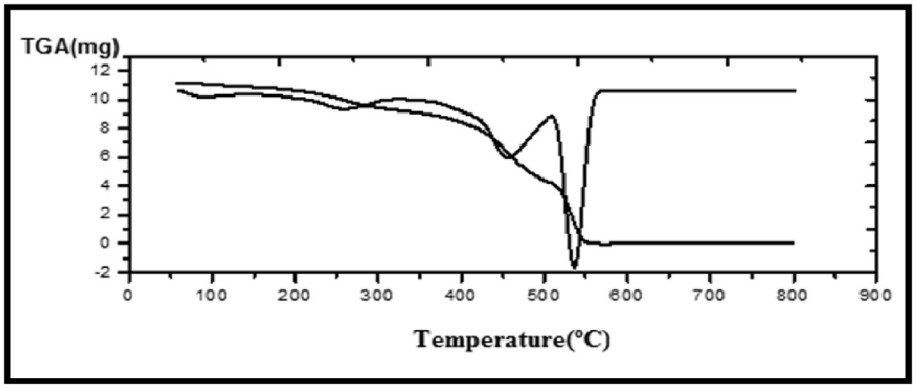

Fig. 1. The TGA-DrTGA curves of $[(L)Ni_2(OAc)_4(H_2O)_2(C_2H_5OH)_2].1.5H_2O$ (**1**).

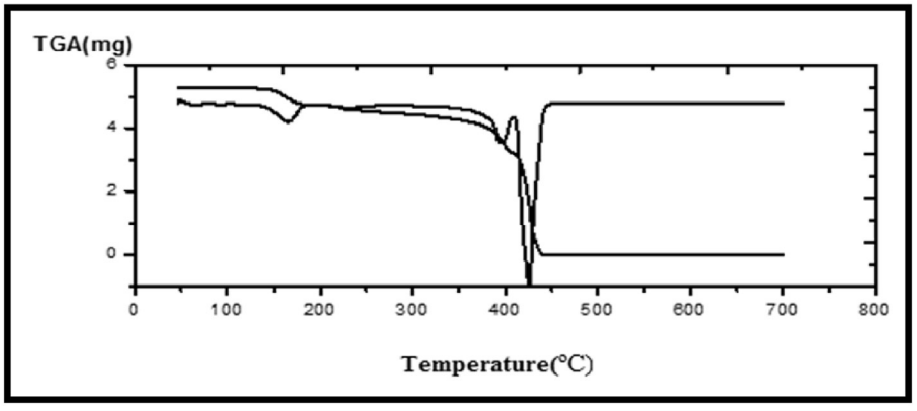

Fig. 2. The TGA-DrTGA curves of $[(L)Ni_2(OAc)_2(8\text{-}HQ)_2(H_2O)_2].0.5C_2H_5OH$ (**4**).

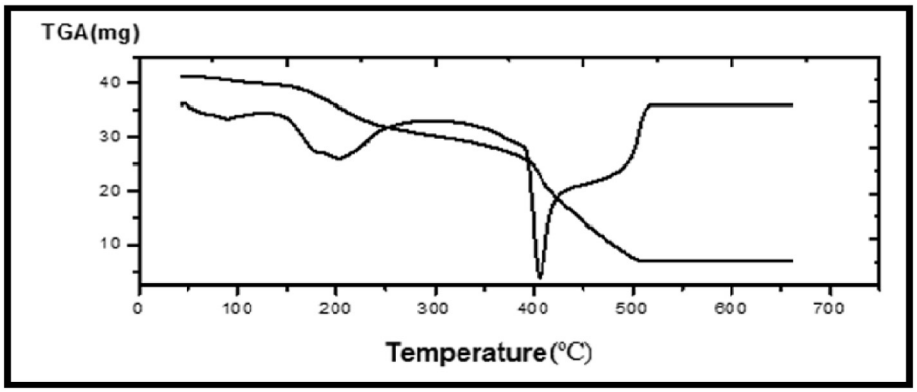

Fig. 3. The TGA-DrTGA curves of $[(L)Co_2(OAc)_4(Amiopy)_2(H_2O)_2].2H_2O$ (**12**).

Table 5
Temperatures of decomposition and the kinetic parameters of complexes.

Complex	Step	N order	T (K)	Δ E (kJ mol^{-1})	ΔH (kJ mol^{-1})	ΔS (kJ $mol^{1}K^{-1}$)	ΔG (kJ mol^{-1})
$[Ni_2(L)(OAc)_4(H_2O)_2(EtOH)_2].1.5H_2O$ **(1)**	1st	1	368	6.12	3.06	−0.255	96.91
	2nd	0.33	524	6.099	1.74	−0.277	146.7
	3rd	0	721	18.13	12.13	−0.264	202.935
$[Ni_2(L)(OAc)_2(8\text{-}HQ)_2(H_2O)_2].0.5EtOH$ **(4)**	1st	1	343	36.22	33.37	−0.143	82.32
	2nd	0.66	435	1.62	−1.996	−0.193	82.37
	3rd	1	518	6.288	1.98	−0.270	143.28
$[Ni_2(L)(OAc)_4(2\text{-}Ampy)_2(H_2O)_2].2.5H_2O$ **(6)**	1st	0.66	373	55.26	52.26	−0.121	97.218
	2nd	1	489	31.59	27.52	−0.210	130.66
$[Co(L)(OAc)_2].H_2O$ **(7)**	1st	1	367	45.54	42.49	−0.146	96.38
	2nd	0.66	496	2.577	−1.546	−0.207	101.16
$[Co_2(L)(OAc)_2(8\text{-}HQ)_2(H_2O)_2]$ **(9)**	1st	1	531	6.258	1.843	−0.260	142.30
$[Co_2(L)(OAc)_4(2\text{-}Ampy)_2(H_2O)_2].2H_2O$ **(12)**	1st	1	363	98.23	95.21	−0.079	123.94
	2nd	0	480	36.05	32.01	−0.194	125.39

3.1.5. Mass spectra

The mass spectral studies of the representative complexes **2**, **7**, **8** and **10** have been performed and the spectra of complexes **7** and **10** are illustrated in Fig. 4. The molecular ion peaks were observed at *m/z* 788 and 735 for complexes **2** and **8,** respectively. This is consistent with showed the molecular ion peaks at *m/z* 788 and 735, respectively, which agree very well with the formula weights of the complexes (F. Wt = 787.6 and 734.6, respectively). For complexes **7** and **10**, the molecular ion peaks were detected at *m/z* 782 and 810, respectively, which is compatible with the calculated formula weights of the non-hydrated complexes $[Co(L)(OAc)_2]$; (F.Wt = 781.7) and [Co(L)(Gly)](OAc); (F.Wt = 810.53).

At last, in the light of the interpretation of analytical and spectral techniques mentioned above, proposed structures of the nickel(II) and cobalt(II) complexes can be summarized in Schemes 1.

3.1.6. XRD analysis

The X-ray diffractograms of the pyridazinone ligand and some of the prepared complexes are shown in Figs. 5 and 6. The patterns and results of XRD suggested that the crystals of the complexes are not perfect but they are between amorphous and crystalline character. The diffractograms and associated data depict the 2θ value for each peak, the relative intensity of the prepared complexes which different from those of the ligand. This result suggests that the metal ions were coordinated to the ligand to form new complexes [62]. Particle sizes of the complexes were calculated using maximum intensity peak by the standard Scherer equation [63]. The calculated values were in the range 20−106 nm.

3.2. Biological studies

3.2.1. Antimicrobial studies

The antimicrobial activity of the Schiff base and its nickel(II) and cobalt(II) complexes was examined towards the subsequent organisms; *E. coli* and *S. typhimurium* (Gram −ve bacteria), *S. aureus* and *B. subtilis* (Gram +ve bacteria), *C. albicans* (yeast) and *A. fumigatus* (fungus) and the obtained results are tabulated in Table 6.

The Schiff base ligand (L) is found ineffective to all bacteria and fungus except it showed lower activety against *Bacillus subtilis*. Metal complexes showed lower activity except complexes **5** and **8**. Complex **5** showed higher activity against *Candida albican*. However, complex **8** has a good influence against all Gram-positive bacteria and *Candida albican* as Yeasts**.**

The prepared complexes showed high activity towerds *Bacillus subtilis* (Fig. 7) are arranged in the following order: **8** > **12** > **7** > **5** > **1** > **4** > **L**. Also, some complexes showed high activity towerds *Candida albican* (Fig. 8) are arranged in the following order: **5** > **8** > **12** > **1**−**7** > **4** > **L**. Higher inhibition zone of metal complexes than those of ligand can be explained on basis of overton's concept and chelation theory.

Overton's concept of cell permeability illustrated that the cell's

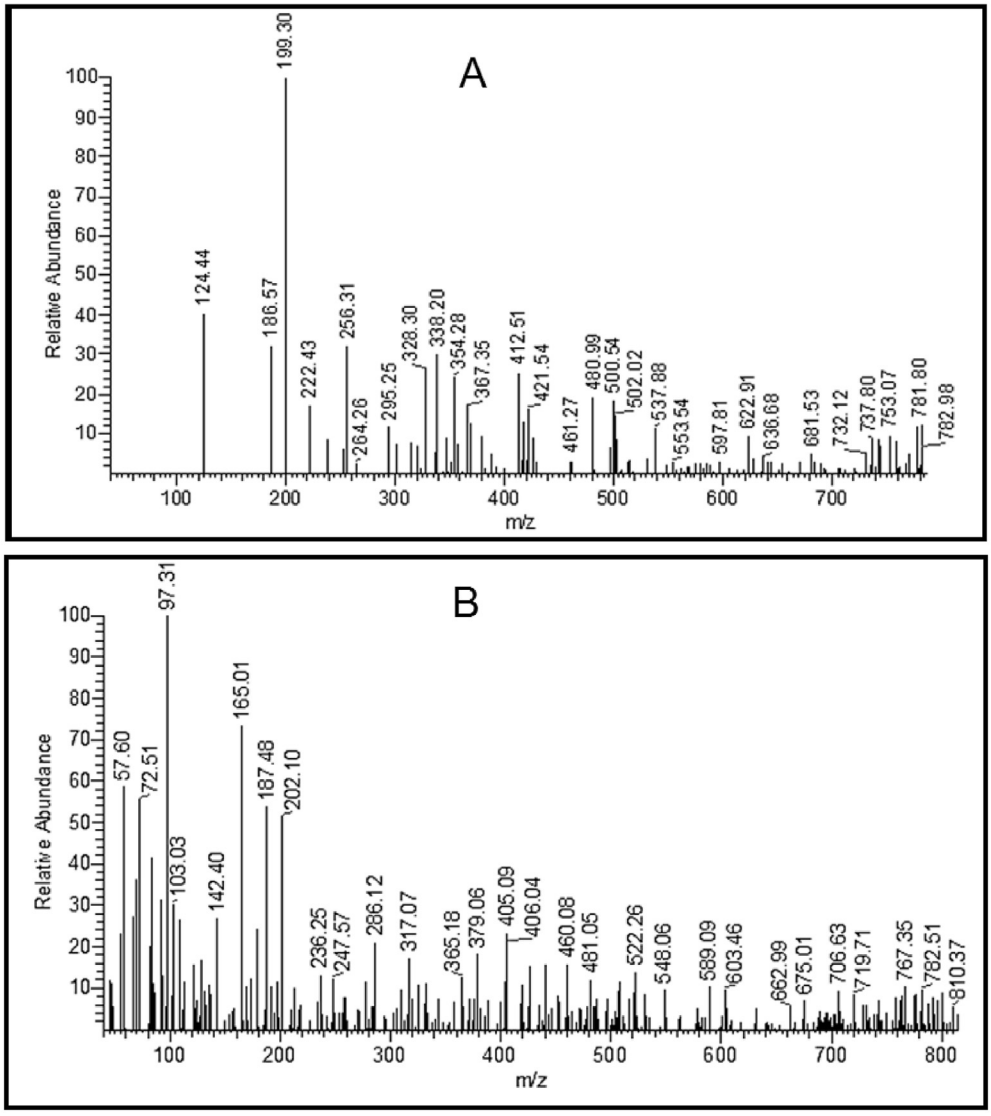

Fig. 4. Mass spectra of the complexes A: $[Co(L)(OAc)_2].H_2O$ (**7**) and B: $[Co(L)(Gly)](OAc).2H_2O$ (**10**).

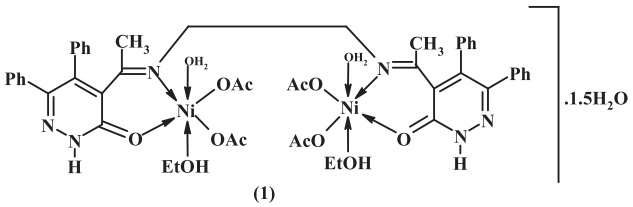

(1)

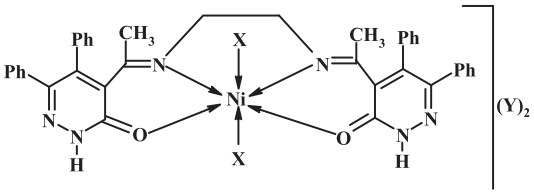

X	Y	Complex
nil	NO_3	**2**
H_2O	ClO_4	**3**

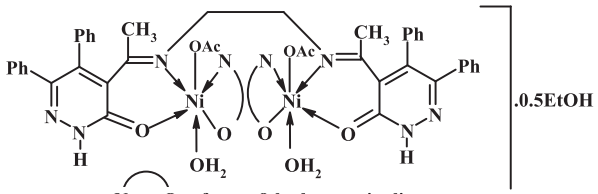

(4)

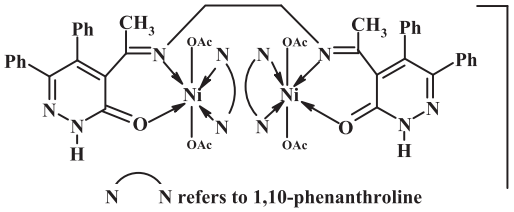

(5)

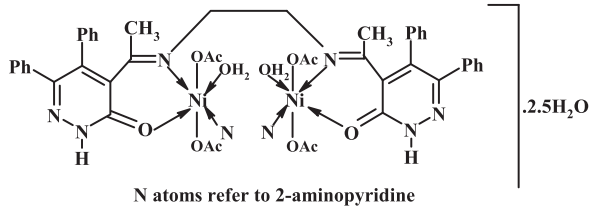

(6)

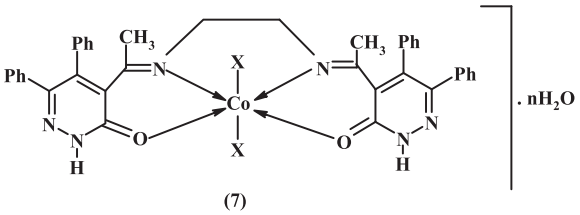

(7)

X	n	Complex
OAc	1	**7**
Cl	nil	**8**

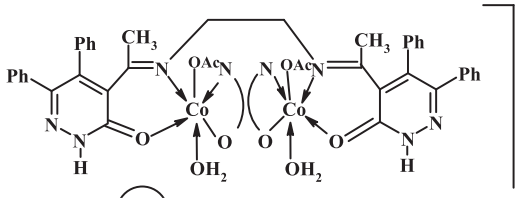

(9)

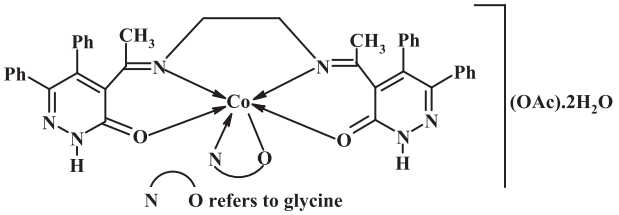

(10)

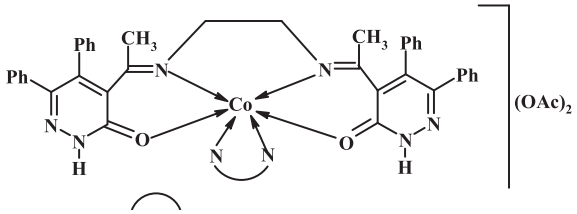

(11)

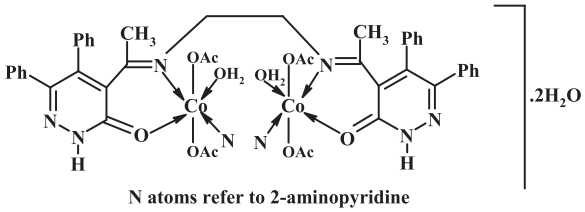

(12)

Scheme 1. Representative structures of the binary and ternary complexes.

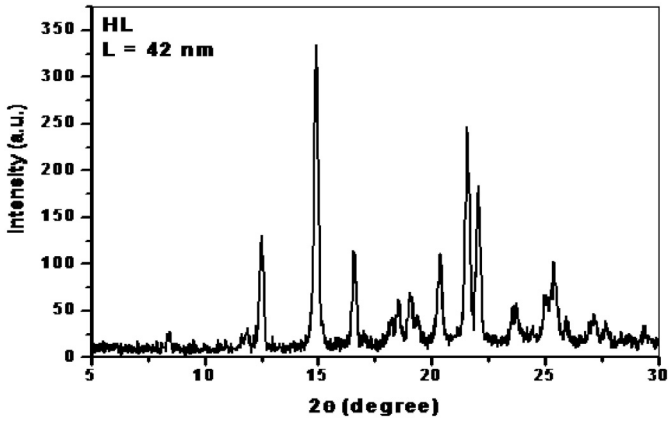

Fig. 5. XRD pattern of the Schiff base Ligand.

the +ve charge of the metal ion with the donor groups). The increasing of delocalization of π-electrons over the whole chelate ring, resulting in an increase in the lipophilicity of the metal complexes. This improved lipophilicity enhances the concentration of complexes in the lipid membrane and limits the multiplicity of microorganisms [64].

3.2.2. Antitumor studies

Some representative Ni(II) and Co(II) complexes (**1**, **4**, **7** and **9**) were checked for their *in vitro* antitumor activity against human cancer cell line liver Carcinoma (HEPG2) and the results are tabulated in Table 7. It was found that complexes **1** and **7** are more active than the free ligand while complexes **4** and **9** showed lower activity than the ligand. The increased conjugation in the Schiff base skeleton as a result of complex-formation [65–67] may be the reason for the higher activity of the complexes compared to that of the Schiff base. In addition to from XRD analysis, the crystal size of present metal complexes with in the nanoscale. This nanocharacter of the present complexes improved the antituomer activity, which facilitates their penetration into tumor cell [63].

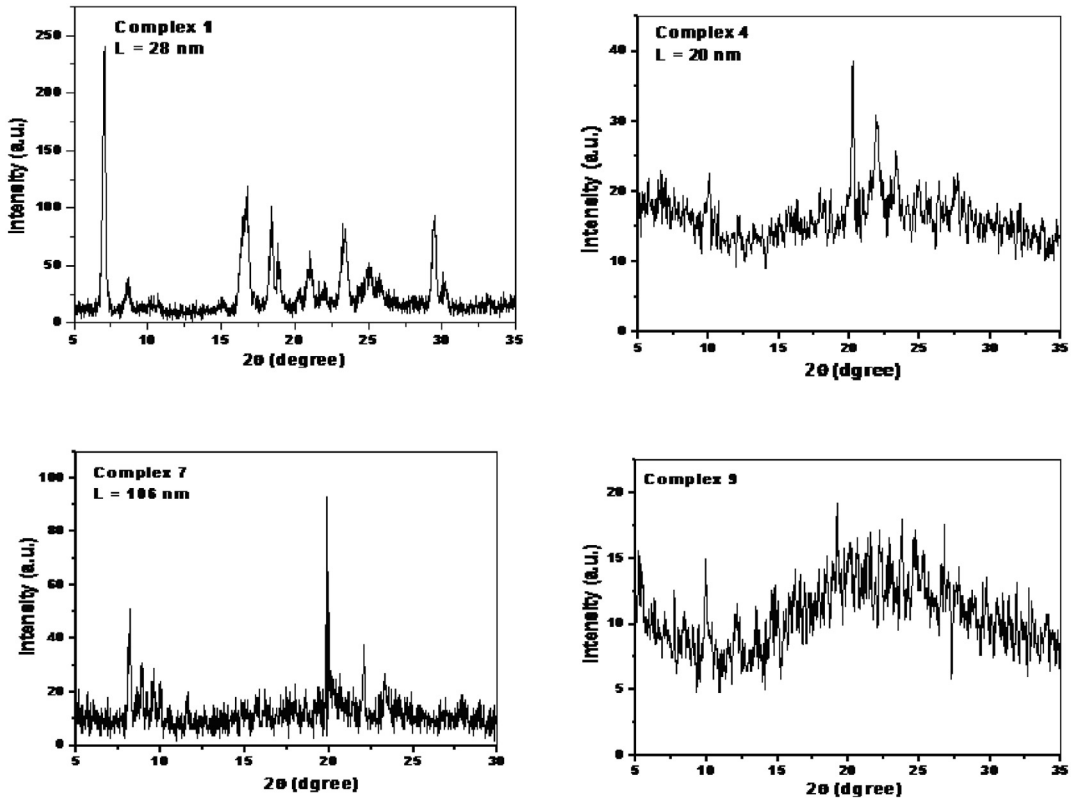

Fig. 6. XRD pattern of metal complexes (**1**, **4**, **7** and **9**).

lipid membrane prefers the passage of just fat-soluble substances, and lipid solubility is an important factor affecting antifungal activity. On complex-formation, when the ion chelates with a chelating agent, its polarity will be greatly reduced (because of the overlap of the chelating agent orbital and the partial sharing of

4. Conclusion

A series of nickel(II) and cobalt(II) Schiff base complexes have been synthesized using different anions. Different analytical and spectroscopic methods were utilized to characterize metal

Table 6
Antimicrobial activity of the ligand and its metal complexes.

Organism	Mean[a] of zone diameter, nearest whole mm.											
	Gram - positive bacteria				Gram - negative bacteria				Yeasts and Fungi[b]			
	Staphylococcus aureus		*Bacillus subtilis*		*Salmonella typhimurium*		*Escherichia coli*		*Candida albicans*		*Aspergillus fumigatus*	
	Concentration											
Sample	1 mg/ml	0.5 mg/ml	1 mg/ml	0.5 mg/ml	1 mg/ml	0.5 mg/ml	1 mg/ml	0.5 mg/ml	1 mg/ml	0.5 mg/ml	1 mg/ml	0.5 mg/ml
L	–	–	9L	7L	–	–	–	–	–	–	–	–
(1) $[Ni_2(L)(OAc)_4(H_2O)_2(EtOH)_2].1.5H_2O$	–	–	15I	12I	–	–	–	–	19I	17I	–	–
(2) $[Ni(L)](NO_3)_2$	–	–	–	–	–	–	–	–	–	–	–	–
(3) $[Ni(L)(H_2O)_2](ClO_4)_2$	–	–	–	–	–	–	–	–	–	–	–	–
(4) $[Ni_2(L)(OAc)_2(8\text{-}HQ)_2(H_2O)_2].0.5EtOH$	–	–	8L	7L	–	–	–	–	8L	7L	–	–
(5) $[Ni_2(L)(OAc)_4(Phen)_2]$	9L	8L	16I	13I	–	–	10L	8L	28H	23H	–	–
(6) $[Ni_2(L)(OAc)_4(2\text{-}Ampy)_2(H_2O)_2].2.5H_2O$	–	–	10L	8L	–	–	–	–	19I	18I	–	–
(7) $[Co(L)(OAc)_2].H_2O$	14I	12I	18I	16I	11L	8L	10L	8L	12I	9L	–	–
(8) $[Co(L)Cl_2]$	24H	20H	25H	21H	17I	13I	17I	14I	25H	22H	–	–
(9) $[Co_2(L)(OAc)_2(8\text{-}HQ)_2(H_2O)_2]$	–	–	–	–	–	–	–	–	–	–	–	–
(10) $[Co(L)(Gly)](OAc).2H_2O$	–	–	–	–	–	–	–	–	–	–	–	–
(11) $[Co(L)(Phen)](OAc)_2$	–	–	14I	11I	–	–	–	–	17I	15I	–	–
(12) $[Co_2(L)(OAc)_4(2\text{-}Ampy)_2\ (H_2O)_2].2H_2O$	22I	19I	18I	15I	19I	16I	24I	20H	19I	17I	–	–
Control[c]	35	26	35	25	36	28	38	27	35	28	37	26

– = No effect.
L: Low activity = Mean of zone diameter ≤1/3 of mean zone diameter of control.
I: Intermediate activity = Mean of zone diameter ≤2/3 of mean zone diameter of control.
H: High activity = Mean of zone diameter >2/3 of mean zone diameter of control.
[a] Calculated from 3 values.
[b] Identified on the basis of routine cultural, morphological and microscopical characteristics.
[c] Chloramphenicol in the case of Gram-positive bacteria, cephalothin in the case of Gram-negative bacteria and cycloheximide in the case of fungi.

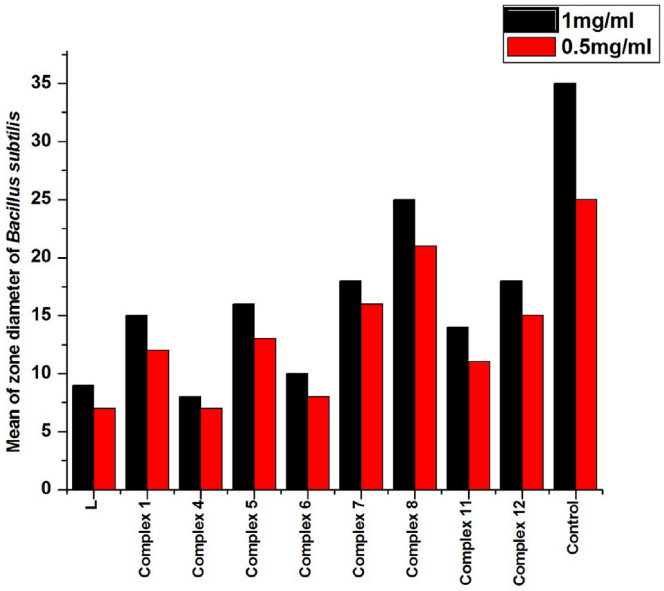

Fig. 7. Relation between the ligand and its metal complexes and their reactivity toward *Bacillus subtilis*.

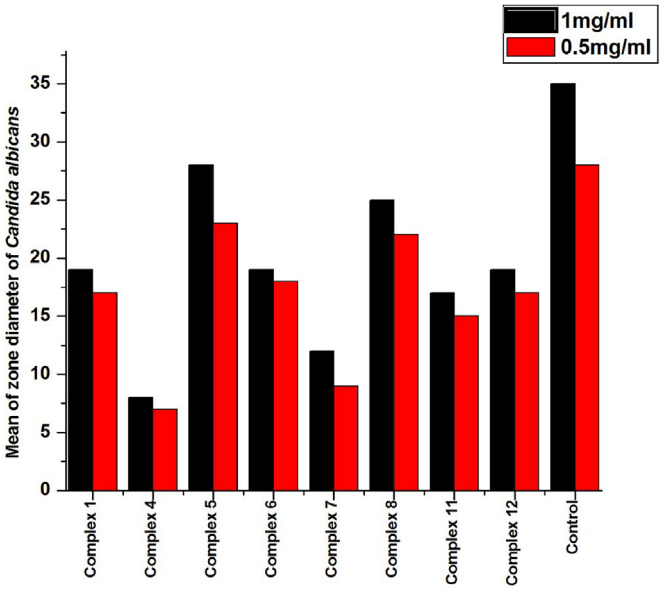

Fig. 8. Relation between the ligand and its metal complexes and their reactivity toward *Candida albicans*.

complexes. The obtained complexes are mono- and binuclear complexes with octahedral and tetrahedral geometry. Coats-Redfern equations were utilized to calculate kinetic and thermodynamic parameters. The Schiff base and its complexes exhibited antimicrobial activity against bacteria and fungi, especially *C. albicans*. The antitumor activity of the Schiff base and its metal complexes was explored against HepG2 cell line where the activity is altered upon complex-formation.

Table 7
Antitumor activity of the Schiff base ligand and its complexes against HepG2 cell line.

Compound	IC_{50} (μg/ml)
L	15.3
$[Ni_2(L)(OAc)_4(H_2O)_2(EtOH)_2].1.5H_2O$ **(1)**	2.94
$[Ni_2(L)(OAc)_2(8\text{-}HQ)_2(H_2O)_2].0.5EtOH$ **(4)**	197
$[Co(L)(OAc)_2].H_2O$ **(7)**	3.78
$[Co_2(L)(OAc)_2(8\text{-}HQ)_2(H_2O)_2]$ **(9)**	405
Doxorubicin	0.47

IC_{50} = inhibition concentration 50%.

Credit author statement

Omima M.I.Adly: Assistant Prof. of inorganic chemistry, Faculty of Education, Ain Shams University. Omima M.I.Adly has supervised several research students that led to M.S. and Ph.D. degrees being awarded in inorganic chemistry. She has participated in more than ten international conferences.

Declaration of competing interest

- The authors declare that they have no conflict of interest.
- This work was not funded from any sources
- All authors at the faculty of education-Ain Shams University are agreeing to submit this work for journal of Molecular Structure.
- Authors whose names appear on the submission have contributed sufficiently to the scientific work and therefore share collective responsibility and accountability for the results.

References

[1] Y.-T. Liu, J. Sheng, D.-W. Yin, H. Xin, X.-M. Yang, Q.-Y. Qiao, Z.-J. Yang, J. Organomet. Chem. 856 (2018) 27.
[2] A. Palanimurugan, A. Kulandaisamy, J. Organomet. Chem. 861 (2018) 263.
[3] T. Thirunavukkarasu, H.A. Sparkes, K. Natarajan, V.G. Gnanasoundari, Inorg. Chim. Acta. 473 (2018) 255.
[4] B. Iftikhar, K. Javed, M.S.U. Khan, Z. Akhter, B. Mirza, V. Mckee, J. Mol. Struct. 1155 (2018) 337.
[5] W.M. Abdou, N.A. Ganoub, M.A.H. Ismail, E. Sabry, R.F. Barghash, A. Geronikaki, Arab. J. Chem. 10 (2017) 1084.
[6] A.A. Shanty, P.V. Mohanan, Spectrochim. Acta 192 (2018) 181.
[7] M. Jafari, M. Salehi, M. Kubicki, A. Arab, A. Khaleghian, Inorg. Chim. Acta. 462 (2017) 329.
[8] T.C. Amaral, F.B. Miguel, M.R.C. Couri, P.P. Corbi, M.A. Carvalho, D.L. Campos, F.R. Pavan, A. Cuin, Polyhedron 146 (2018) 166.
[9] H. Zafar, A. Ahmad, A.U. Khan, T.A. Khan, J. Mol. Struct. 1097 (2015) 129.
[10] E.M. Njogu, B. Omondi, V.O. Nyamori, J. Mol. Struct. 1135 (2017) 118.
[11] H.F. Abd El-Halim, G.G. Mohamed, E.A.M. Khalil, J. Mol. Struct. 1146 (2017) 153.
[12] H. Keypour, M. Mahmoudabadi, A. Shooshtari, M. Bayat, F. Mohsenzadeh, R.W. Gable, J. Mol. Struct. 1155 (2018) 196.
[13] P. Ghorai, R. Saha, S. Bhuiya, S. Das, P. Brandão, D. Ghosh, T. Bhaumik, P. Bandyopadhyay, D. Chattopadhyay, A. Saha, Polyhedron 141 (2018) 153.
[14] M.A. Ewida, D.A. Abou El Ella, D.S. Lasheen, H.A. Ewida, Y.I. El-Gazzar, H.I. El-Subbagh, Bioorg. Chem. 74 (2017) 228.
[15] M.S. Mohamed, A.O. Abdelhamid, F.M. Almutairi, A.G. Ali, M.K. Bishr, Bioorg. Med. Chem. 26 (2018) 623.
[16] Z. Wang, M. Wang, X. Yao, Y. Li, J. Tan, L. Wang, W. Qiao, Y. Geng, Y. Liu, Q. Wang, Eur. J. Med. Chem. 54 (2012) 33.
[17] D. Li, P. Zhan, H. Liu, C. Pannecouque, J. Balzarini, E.D. Clercq, X. Liu, Bioorg. Med. Chem. 21 (2013) 2128.
[18] D. Mantu, M.C. Luca, C. Moldoveanu, G. Zbancioc, I.I. Mangalagiu, Eur. J. Med. Chem. 45 (2010) 5164.
[19] L.Z. Bendjeddou, N. Loaec, B. Villiers, E. Prina, G.F. Spath, H. Galons, L. Meijer, N. Oumata, Eur. J. Med. Chem. 125 (2017) 696.
[20] N. Ghareb, H.A. Elshihawy, M.M. Abdel-Daim, M.A. Helal, Bioorg. Med. Chem. Lett 27 (2017) 2377.
[21] L.-P. Guan, X. Suib, X.-Q. Deng, Y.-C. Quan, Z.-S. Quan, Eur. J. Med. Chem. 45 (2010) 1746.
[22] R. Barbaro, L. Betti, M. Botta, F. Corelli, G. Giannaccini, L. Maccari, F. Manetti, G. Strappaghetti, S. Corsano, J. Med. Chem. 44 (2001) 2118.
[23] N.G. Kandile, M.I. Mohamed, H. Zaky, H.M. Mohamed, Eur. J. Med. Chem. 44 (2009) 1989.
[24] C. Lamberth, S. Trah, S. Wendeborn, R. Dumeunier, M. Courbot, J. Godwin, P. Schneiter, Bioorg. Med. Chem. 20 (2012) 2803.
[25] N.A. Khalil, E.M. Ahmed, K.O. Mohamed, Y.M. Nissan, S.A. Zaitone, Bioorg. Med. Chem. 22 (2014) 2080.
[26] K.H. Reddy, P.S. Reddy, P.R. Babu, Trans. Met. Chem. 25 (2000) 505.
[27] J.D. Joshi, S. Sharma, G. Patel, J.J. Vora, Synth. React. Inorg. Met. Org. Chem. 32 (2002) 1729.
[28] M. Shebl, O.M.I. Adly, E.M. Abdelrhman, B.A. El-Shetary, J. Mol. Struct. 1145 (2017) 329.
[29] F.E. Mabbs, D.I. Machin, Magnetism and Transition Metal Complexes, Chapman and Hall, London, 1973.
[30] V.P. Schmidt, J. Druey, Helv. Chim. Acta 37 (1954) 134.
[31] (a) A.U. Rahman, M.I. Choudhary, W.J. Thomsen, Bioassay Techniques for Drug Development, Harwood Academic Publishers, The Netherlands, 2001;
(b) K.M. Khan, Z.S. Saify, A.K. Zeesha, M. Ahmed, M. Saeed, M. Schick, H.J. Kohlbau, W. Voelter, Arzneim. Forsch. 50 (2000) 915.
[32] (a) T. Mosmann, J. Immunol. Methods 65 (1983) 55;
(b) S.M. Gomha, S.M. Riyadh, E.A. Mahmmoud, M.M. Elaasser, Heteocycles 91 (2015) 1227.
[33] M. Sönmez, İ. Berber, E. Akbaş, Eur. J. Med. Chem. 41 (2006) 101.
[34] K. Nakamoto, Infrared and Raman Spectra of Inorganic and Coordination Compounds, fifth ed., John Wiley and Sons, New York, 1997.
[35] G.M. Abu El-Reash, O.A. El-Gammal, A.H. Radwan, Spectrochim. Acta 121 (2014) 259.
[36] L. Bellamy, The IR Spectra of Complex Molecule, Methuen, London, 1985.
[37] N.T. Madhu, P.K. Radhakrichnan, Synth. React. Inorg. Met. Org. Chem. 31 (2001) 315.
[38] U. El-Ayaan, I.M. Gabr, Spectrochim. Acta 67 (2007) 263.
[39] A. Taha, Spectrochim. Acta 59 (2003) 1611.
[40] M. Shebl, O.M.I. Adly, A. Taha, N.N. Elabd, J. Mol. Struct. 1147 (2017) 438.
[41] H. Keypour, H. Goudarziafshar, A.K. Brisdon, R.G. Pritchard, M. Rezaeivala, Inorg. Chim. Acta. 361 (2008) 1415.
[42] M. Shebl, M.A. El-ghamry, S.M.E. Khalil, M.A.A. Kishk, Spectrochim. Acta 126 (2014) 232.
[43] A.M. Shaker, A.M. Awad, L.A.E. Nassr, Synth. React. Inorg. Met. Org. Chem. 33 (2003) 103.
[44] S. Shobana, J. Dharmaraja, S. Selvaraj, Spectrochim. Acta 107 (2013) 117.
[45] P. Teyssie, J.J. Charette, Spectrochim. Acta 19 (1963) 1407.
[46] Z.H. Abd El-Wahab, M.M. Mashaly, A.A. Salman, B.A. El-Shetary, A.A. Faheim, Spectrochim. Acta 60 (2004) 2861.
[47] M. Gaber, A.M. Khedr, M.A. Mansour, M. Elsharkawy, Appl. Organomet. Chem. 32 (2018) e4606.
[48] W.J. Geary, Coord. Chem. Rev. 7 (1971) 81.
[49] F.A. Cotton, G. Wilkinson, Advanced Inorganic Chemistry. A Comprehensive Text, fourth ed., John Wiley and Sons, New York, 1986.
[50] N.N. Greenwood, A. Earnshaw, Chemistry of the Elements, Pergamon Press, New York, 1984.
[52] O.M.I. Adly, Spectrochim. Acta 79 (2011) 1295.
[53] M. Shebl, J. Mol. Struct. 1128 (2017) 79.
[54] K.A.R. Salib, S.L. Stefan, S.M. Abu El-Wafa, H.F. El-Shafiy, Synth. React. Inorg. Met. Org. Chem. 31 (2001) 895.
[55] S.M. Morgan, M.A. Diab, A.Z. El-Sonbati, Appl. Organomet. Chem. 32 (2018), e4305.
[56] M. Shebl, O.M.I. Adly, H.F. El-Shafiy, S.M.E. Khalil, A. Taha, M.A.N. Mahdi, J. Mol. Struct. 1134 (2017) 649.
[57] M. Tavassoli, M. Montazerozohori, A. Masoudiasl, Z. Akbari, Th Doert, E.M. Vazquez Lopez, S.J. Fatemi, Polyhedron 176 (2020) 114287.
[58] A.W. Coats, J.P. Redfern, Nature 201 (1964) 68.
[59] A.H.M. Siddaligaiah, S.G. Naik, J. Mol. Struct. 582 (2002) 129.
[60] C.R. Vinodkumar, M.K.M. Nair, P.K. Radhakrishnan, J. Therm. Anal. Calorim. 61 (2000) 143.
[61] H. Masuda, K. Miyokawa, I. Masuda, Thermochim. Acta 84 (1985) 331.
[62] H.F. El-Shafiy, M. Saif, M.M. Mashaly, S. Abdel Halim, Mohamed F. Eid, A.I. Nabeel, R. Fouad, J. Mol. Struct. 1147 (2017) 452.
[63] M. Saif, H.F. El-Shafiy, M.M. Mashaly, M.F. Eid, A.I. Nabeel, R. Fouad, J. Mol. Struct. 1155 (2018) 765.
[64] (a) B. Murukan, K. Mohanan, J. Enzym. Inhib. Med. Chem. 22 (2007) 65;
(b) M. Imran, L. Mitu, S. Latif, Z. Mahmood, I. Naimat, S.S. Zaman, S. Fatima, J. Serb. Chem. Soc. 75 (2010) 1075.
[65] H.F. El-Shafiy, M. Shebl, J. Mol. Struct. 1194 (2019) 187.
[66] M. Shebl, S.M.E. Khalil, M.A.A. Kishk, D.M. El-Mekkawi, M. Saif, Appl. Organomet. Chem. 33 (2019) e5147.
[67] K. Dhahagani, S.M. Kumar, G. Chakkaravarthi, K. Anitha, J. Rajesh, A. Ramu, G. Rajagopal, Spectrochim. Acta A. 117 (2014) 87.